8. Oxidation power of chlorophylls

O_2 on earth is generated by water oxidation in the Mn-cluster of the photosynthetic protein-pigment complex, PSII. Charge separation leads to formation of an oxidized positively-charged radical $P680^+$. In intact PSII, $P680^+$ is re-reduced by the redox-active tyrosine D1-Tyr161 (Y_Z), which is subsequently reduced by ET from the Mn-cluster (Figure 1-2). Sequential excitations of P680 drive the redox state of the Mn-cluster from the lowest S0 to the highest oxidized state S4. O_2 evolves during the S3 to S0 transition via the transiently S4 state, which has not been resolved in spectroscopic studies (reviewed in ref. (Goussias et al., 2002)). Thus, as an electron donor to the Mn-cluster, E_m of P680 should be unusually high, which was estimated to be ~+1100-1300 mV in recent kinetic studies (Rappaport et al., 2002) and computations (Ishikita and Knapp, 2005a; Ishikita et al., 2005b).

D1/D2 protein of PSII has a large structural similarity with subunit L/M of bRC (Michel and Deisenhofer, 1988) (Figure 1-2 and 1-3). The four Chl*a* $P_{D1/D2}$ and $Chl_{D1/D2}$ in PSII is conserved as four BChl*a* $P_{L/M}$ and $B_{L/M}$, respectively. In bRC from *Rb. sphaeroide*s the pigment P870 corresponds to P680 of PSII. However, the E_m(P870) has been measured to be +500 mV (Williams et al., 1992), which is at least by 600 mV lower than E_m(P680). Unlike the weak coupling of Chl*a* in the D1/D2 proteins of PSII, the electronic coupling between P_L and P_M is strong because of the perfect overlap of the BChl*a* Rings-I between P_L and P_M. Therefore, the E_m(P870) of +500 mV (Williams et al., 1992) is considered to refer to the energy level of the highest molecular orbital (HOMO) of the dimer BChl*a*, which is formed by the π-π conjugation of the each HOMO of P_L and P_M. Indeed, the $E_m(P_L)$ ($\neq E_m$(P870)) is +640 mV (Allen et al., 1996), indicating that the electronic coupling lowers the E_m(P870) by ~140 mV with respect to $E_m(P_L)$. Note that the value of +640 mV for $E_m(P_L)$ was obtained from the H(M202)L mutant (heterodimer) bRC, in which the BChl*a* at P_M is substituted by BPhe*oa* due to the elimination of the His ligand at M202 (Allen et al., 1996).

Nevertheless, the dramatic E_m difference of at least ~600 mV between P680 and P870 cannot be explained only by the strong electronic coupling in P870. Although E_m(BChl*a*) in CH_2Cl_2 (Fajer et al., 1975) are by 160 mV lower than r E_m(Chl*a*) in CH_2Cl_2 (Fajer et al., 1982; Maggiora et al., 1985), there is still a 440 mV difference unexplained. In this regard, it should also be noted that the pigment P700 in photosystem I (PSI) possesses the E_m of ~+500 mV (reviewed in ref. (Brettel, 1997), Figure 1-3). In PSI four Chl*a* $P_{A/B}$ and $A_{-1A/B}$ are located in subunit PsaA/PsaB as a corresponding position of $P_{L/M}$ and $B_{L/M}$ in bRC ($P_{D1/D2}$ and $Chl_{D1/D2}$ in PSII). P700 mainly consists of a pair of Chl*a* $P_{A/B}$ (reviewed in ref. (Webber and Lubitz, 2001)). Despite of Chl*a* at a position of $P_{A/B}$ and $P_{D1/D2}$, E_m(P700) is by ~600 mV lower than E_m(P680).

8.1. E_m(P870) in bRC

8.1.1. Monomer $E_m(P_{L/M})$ in bRC

In the wild type bRC, E_m(P870) was measured to be +500 mV (Williams et al., 1992). Solving the LPB equation to evaluate electrostatic energies for the three crystal structures of the wild type bRC, we computed average values of +635±12 mV for $E_m(P_L)$ and +660±14 mV for $E_m(P_M)$ (Figure 8-1-1) (Ishikita et al., 2005c).

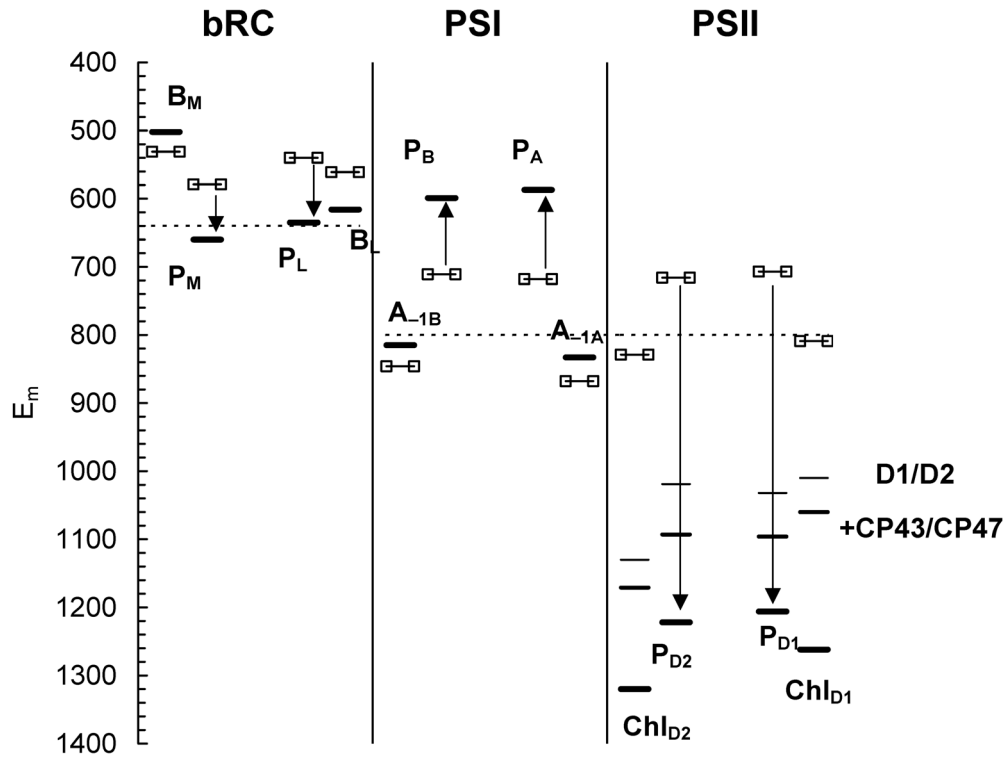

Figure 8-1-1. Calculated E_m(BChl*a*) in bRC and E_m(Chl*a*) in PSI and PSII (solid lines). The dotted lines indicate the reference values in CH_2Cl_2, which are E_m(BChl*a*) = +640 mV (Fajer et al., 1975) and E_m(Chl*a* = +800 mV (Fajer et al., 1982; Maggiora et al., 1985). Thin solid lines with open squares at the both edges refer to E_m(BChl*a*) and E_m(Chl*a*) calculated in the absence of atomic charges in the protein. The calculated E_m(Chl*a*) for the D1/D2 and the D1/D2CP43/CP47 cores of PSII are indicated with thin solid lines.

It has been suggested that the π-π interactions of the (B)Chl*a* are likely to be stronger in P870 than that in P700 because of large overlap of the BChl*a* rings-I between P_L and P_M compared with a negligible overlap in PSI (Jordan et al., 2001). Thus, we assume that the difference between E_m(P870) and $E_m(P_L)$ / $E_m(P_M)$ might be larger than that between E_m(P700) and $E_m(P_A)$ / $E_m(P_B)$. To estimate the effect of electronic coupling on E_m(P870), we also calculated $E_m(P_L)$ for the H(M202)L heterodimer bRC. In the heterodimer bRC P_M is replaced by BPheo*a* due to the lack of His-M202 serving as ligand for P_M, such that after charge separation the cationic state is localized on the remaining monomer BChl*a* at P_L. Therefore, the measured E_m(P870) = +640 mV (Allen et al., 1996) in the heterodimer bRC has been assumed to be the actual $E_m(P_L)$ for the wild type bRC when the electronic coupling between P_L and P_M is absent (Ivancich et al., 1998).

Based on the crystal structure of the heterodimer bRC, we obtained the calculated $E_m(P_L)$ to be +639 mV, which agrees with measured value of +640 mV in the heterodimer bRC (Allen et al., 1996). Indeed, the average value of +635 mV calculated for $E_m(P_L)$ in the different crystal structures of wild type bRC from *Rb. sphaeroides* adopts virtually the same value, and even the average value of +660 for $E_m(P_M)$ is at the same level presumably due to a relatively similar protein environment.

8.1.2. Dimer E_m(P870) in bRC

To account for the measured E_m(P870) = +495 mV, Ivancich *et al*. (Ivancich et al., 1998) estimated $E_m(P_{L/M})$ to be +680/+800 mV based on the ratio of $\rho(P_L)/\rho(P_M)$ of

2.56 for spin density (i.e. $\rho(P_L) : \rho(P_M) = 0.72 : 0.28$) and the electronic coupling of 240 meV. The most plausible explanation for the significantly higher value of +800 mV for $E_m(P_M)$ by Ivancich *et al*. with respect to our calculated value of +660 mV is likely the counter effect on P_M due to the positive charge localized on P_L as a consequence of the charge distribution, mostly being delocalized on P_L. The large amount of positive charge delocalized on P_L should result in a significant up-shift of $E_m(P_M)$. To check this effect, we recalculated $E_m(P_L)$ with $P_M^{0.28+}$ ($E_A(P_L)$) and $E_m(P_M)$ with $P_L^{0.72+}$ ($E_A(P_M)$), where the atomic partial charges of $P_M^{0.28+}$ and $P_L^{0.72+}$ were estimated by linear interpolation between P_M^0 / P_M^+ and P_L^0 / P_L^+, respectively. We obtained $E_A(P_L)$=+688±7 and $E_A(P_M)$=+795±4 mV, which is in excellent agreement with the estimated values of +680/+800 mV from Ivancich *et al*. (Ivancich et al., 1998).

8.2. E_m(P700) in PSI

8.2.1. Monomer $E_m(P_{A/B})$ in PSI

The calculated $E_m(P_{A/B})$ are +587/+599 mV (Figure 8-1-1). E_m(P700) has been experimentally measured to be ~+500 mV (reviewed in ref. (Brettel, 1997)). Thus, the calculated $E_m(P_{A/B})$ are by ~100 mV higher than experimentally measured E_m(P700). The remaining discrepancy in E_m of 100 mV can be related to the neglect of electronic coupling in our computations. Hence, $P700^+$ may be energetically stabilized relative to either P_A^+ or P_B^+ by weak electronic coupling.

8.3. E_m(P680) in PSII

8.3.1. $E_m(P_{D1/D2})$ and $E_m(Chl_{D1/D2})$ in PSII

The calculated $E_m(P_{D1/D2})$ are +1206/+1222 mV and the calculated $E_m(Chl_{D1/D2})$ are +1262/+1320 mV (Figure 8-1-1). These E_m values are consistent with the estimated value of ~1260 mV for E_m(P680) by Rappaport et al. (Rappaport et al., 2002) and earlier computations (Ishikita and Knapp, 2005a; Ishikita et al., 2005b) based on the 3.2 Å (Biesiadka et al., 2004) and 3.5 Å-structures (Ferreira et al., 2004). The calculated $E_m(Chl_{D1/D2})$ are higher than the calculated $E_m(P_{D1/D2})$. Especially, the calculated $E_m(Chl_{D2})$ is considerably higher than the E_m for the other three Chl*a*, indicating that the cationic state $P680^+$ is most likely not localized at Chl_{D2}.

According to the observation from FTIR (Noguchi et al., 1998) or UV-VIS absorption spectra of the $P_{D1/D2}$-axial-ligand mutant (Diner et al., 2001), the positive charge is delocalized over the $P_{D1/D2}$ dimer as a consequence of charge separation. On the other hand, it has been proposed that the electronic excitation of a multimer of Chl*a* in PSII evolves initially to the charge separated state $P_{D1/D2}{}^0Chl_{D1}{}^+Pheo_{D1}{}^-$ (Dekker and van Grondelle, 2000; Prokhorenko and Holzwarth, 2000). The charge separated state in PSII is further stabilized by transferring the positive charge from Chl_{D1} to $P_{D1/D2}$ leading to $P_{D1/D2}{}^+Chl_{D1}{}^0Pheo_{D1}{}^-$ with a time constant of ~25 ps (Prokhorenko and Holzwarth, 2000). Therefore, the transfer of the positive charge from Chl_{D1} to $P_{D1/D2}$ was proposed to be approximately isoenergetic (Dekker and van Grondelle, 2000). The calculated $E_m(Chl_{D1})$ are by 40-56 mV (equivalent to ~2*k*T) higher than the calculated $E_m(P_{D1/D2})$, which is in agreement with these proposed energetics (Dekker and van Grondelle, 2000; Prokhorenko and Holzwarth, 2000). According to the calculated E_m(Chl*a*) in PSII, under stationary conditions the positive charge is probably localized on $P_{D1/D2}$, as proposed in UV-VIS spectroscopic studies (Noguchi et al., 1998; Diner et al., 2001).

8.3.2. Comparison of $E_m(Chl_{D1/D2})$ with $E_m(B_{L/M})$ and $E_m(A_{-1A/B})$

In PSI, the calculated $E_m(A_{-1A/B})$ are +833/+815 mV (Figure 8-1-1), which are by 220-250 mV higher than those calculated for $P_{A/B}$. In PSII, the corresponding E_m difference between $P_{D1/D2}$ and $Chl_{D1/D2}$ are 60-100 mV, implying that the HOMO of the four Chl*a* in PSII are in a smaller free energy range than those in PSI. This also indicates that in PSI a cationic state should predominantly appear on $P_{A/B}$ but not on $A_{-1A/B}$, which is consistent with the experimental observation that the cationic state is predominantly localized on P_B (reviewed in ref. (Webber and Lubitz, 2001)).

In bRC, the calculated $E_m(B_{L/M})$ are +616±20/+502±11 mV (Figure 8-1-1). Regardless of the structural similarity between the D1/D2 proteins of PSII and the L/M subunits of bRC, the redox pattern of the calculated E_m levels of the four center (B)Chl*a* are quite different. First, in PSII the calculated E_m for the accessory Chl*a* is higher than that for the (pseudo-)dimer Chl*a*, while in bRC the situation is opposite. A major factor responsible for this discrepancy is the absence/presence of the His ligand for the accessory Chl*a*/BChl*a* in PSII/bRC, which accounts for an E_m difference of ~60 mV in the protein environment (~100 mV in aqueous solution, see Method section). Second, in PSII the calculated $E_m(Chl_{D2})$ is the highest among the E_m of the four center Chl*a*, while in bRC the corresponding calculated $E_m(B_M)$ is the lowest. This may be in conflict with the fact that in bRC the positive charge is delocalized over $P_{L/M}$ (Ivancich et al., 1998). Nevertheless, it is probable that due to the much weaker electronic coupling between the dimer and accessory BChl*a*, the positive charge is energetically stabilized on $P_{L/M}$ rather than on B_M.

Table 8-4-1. Influence on cofactor/protein charges on E_m(BChl*a*) and E_m(Chl*a*) [mV].

	bRC				**PsaA/PsaB**				**D1/D2**			
	M		**L**		**B**		**A**		**D2**		**D1**	
	B_M	P_M	P_L	B_L	A_{-1B}	P_B	P_A	A_{-1A}	Chl_{D2}	P_{D2}	P_{D1}	Chl_{D1}
a) cofactor	–13	7	1	–15	21	–57	–83	27	103	123	237	206
b) side-chain	–38	–19	35	47	–121	–84	–85	–123	48	–12	–135	–85
c) backbone	22	93	59	23	71	40	43	62	150	192	223	80
total	–29	81	95	55	–29	–101	–125	–34	301	303	325	201

8.4. What shifts E_m(P680) in PSII to such high values?

8.4.1. Overview of the 600 mV E_m difference between $P_{D1/D2}$ and $P_{A/B}$

(a) 200 mV from subunits. Upon the removal of all the subunits except for D1/D2 of PSII (i.e. the D1/D2 core), the calculated $E_m(P_{D1/D2})$ is down-shifted to +1032/1019 mV (Figure 8-1-1), indicating that 170-200 mV of the 600 mV difference between $E_m(P_{D1/D2})$ and $E_m(P_{A/B})$ originates from the atomic charges and protein dielectric volume of all PSII subunits except for D1/D2. In the D1/D2/CP43/CP47 core of PSII, the calculated $E_m(P_{D1/D2})$ is +1096/1093 mV, resulting in an up-shift of 64/74 mV relative to the D1/D2 core. Nevertheless, these $E_m(P_{D1/D2})$ are still significantly higher than $E_m(P_{A/B})$ = +587/599 mV calculated for the native PSI complex ($E_m(P_{A/B})$ = +593/610 mV for the PsaA/PsaB core). Therefore, in the following part we focus on D1/D2 core, the simplified PSII system.

(b) ~0mV from dielectric volume. One of the remarkable findings is that the protein dielectric volume does not discriminate the E_m values of the RC Chl*a* between PSI and

PSII. This is indicated by the same E_m(Chl*a*) levels calculated in absence of all atomic charges from the protein/cofactor complexes (Figure 8-1-1). Thus, there is no specific difference in the protein dielectric volume between D1/D2 and PsaA/PsaB, as proposed in ref. (Rutherford and Faller, 2003).

(c) 400-450 mV from atomic charge. The majority of the 600 mV E_m difference between $P_{D1/D2}$ and $P_{A/B}$ originates from the protein atomic charges. They are responsible for a dramatic up-shift of 325/303 mV for $E_m(P_{D1/D2})$ in PSII, as opposed to a down-shift of 125/101 mV for $E_m(P_{A/B})$ in PSI. Hence, the atomic charge distribution of the proteins yield a net E_m difference of 400-450 mV between $P_{D1/D2}$ and $P_{A/B}$ (Table 8-4-1).

8.4.2. Side-chain charges in PSII

Occasionally, it was proposed that specific side-chains in PSII near to P680 may be responsible for the up-shift in E_m(P680). In the present study, D2-Arg180 up-shifts the E_m(Chl*a*) in PSII most significantly as proposed previously (Manna et al., 1998; Mulkidjanian, 1999; Ishikita et al., 2005b). This residue up-shifts $E_m(P_{D2})$ and $E_m(Chl_{D2})$ by ~70 mV more than the corresponding E_m(Chl*a*) of D1. The symmetry related residue on the D1 side is the uncharged D1-Asn181, which essentially is not shifting $E_m(P_{D1/D2})$ (Ishikita et al., 2005c). At a structurally similar position in bRC exist a pair of basic residues Arg-L135/Arg-M164, which are the closest residues to $B_{L/M}$ (Supporting Table S4). Thus, the absence of the basic residue on the D1 side of PSII is one of the main factors that up-shift $E_m(Chl_{D2})$ relative to $E_m(Chl_{D1})$.

In PSII there is a considerable side-chain down-shift of $E_m(Chl_{D1})$ by 130 mV relative to $E_m(Chl_{D2})$. Contrary, in bRC the side-chains lead to a down-shift $E_m(B_M)$ by 85 mV relative to $E_m(B_L)$ (Table 8-4-1). The presence of D2-Arg180 on the D2 side is significantly related to the former relative shift. In the bRC case, two important factors need to be considered:

(i) There are seven acidic residues (M88, 95, 100, 111, 173, 184 and 292) on the periplasmic M side of bRC, while on the periplasmic L side there are only four acidic residues (L72, 155, 257 and 261). On both sides, the same number of three basic residues are present. These are M87, M110, M164 and L82, L135, L268. Thus, the periplasmic M side is richer in negative charges than the periplasmic L side, giving rise to ~40 mV down-shift in $E_m(B_M)$ relative to $E_m(B_L)$ (Ishikita et al., 2005c). This contrasts with PSII where, due to the presence of the positively-charged Mn-cluster, more acidic residues are on the D1 than D2 side (Loll et al., 2005). Thus, the distribution of acidic and basic residues is completely opposite between L/M of bRC and D1/D2 of PSII.

(ii) On the L side, in the immediate vicinity of P_L and B_L there is a Tyr (Tyr-M210). The residue, symmetry related to Tyr-M210, is the non-polar Phe-L181. These two residues were suggested to play an important role in the functional asymmetry of the primary ET event between the L and M sides (A-branch/B-branch) (Jones et al., 1994; Beekman et al., 1996). In the present computation, Phe-L181 has essentially no influence on the E_m for all BChl*a*. On the other hand, Tyr-M210 has no significant influence on $E_m(B_M)$. However, Tyr-M210 down-shifts $E_m(P_L)$ by 20 mV and simultaneously up-shifts $E_m(B_L)$ by ~30 mV, yielding an E_m difference of ~50 mV (~30 mV) between P_L and B_L (B_L and B_M) (Ishikita et al., 2005c). Notably, a polar residue corresponding to Tyr-M210 in bRC is absent in PSII (D2-Leu205).

8.4.3. Protonation patterns of titratable residues in PSII

Although some residues in PSII up-shift the E_m(Chl*a*) considerably, the average

up-shifts by side-chains for $E_m(P_{D1/D2})$ and $E_m(Chl_{D1/D2})$ are in the same range as those calculated in bRC and PSI (Table 8-4-1), indicating that there is essentially no strong specificity of side-chain arrangements near those Chl*a* in PSII. The unexpectedly small influence of PSII side-chains on E_m(Chl*a*) is partially due to compensating effect from of side-chain deprotonation upon formation of the Chla^+ states. Specifically, upon formation of P_{D1}^+ or Chl_{D1}^+, we observe deprotonation of D2-Lys317 by 0.4-0.5 H^+. The deprotonation of D2-Lys317 is weaker upon Chla^+ formation on the D2 side (by 0.1-0.3 H^+). Since D2-Lys317 is proposed to participate in the exit pathway of protons generated from water oxidation (Barber et al., 2004; Ferreira et al., 2004; Iwata and Barber, 2004), our result implies an electrostatic link between these Chl*a* and the proton exit pathway.

D2-His61 shows deprotonation by 0.2 H^+ or 0.3 H^+ upon formation of P_{D2}^+ or Chl_{D2}^+, respectively. The role of D2-His61 is unclear. The symmetrical counterpart of this residue is the acidic D1-Asp61 (Chu and Debus, 1995; Clausen et al., 2004), which is very close to the Mn-cluster and belongs to the hydrophilic channel leading to the lumenal bulk surface (Barber et al., 2004; Ferreira et al., 2004; Iwata and Barber, 2004). Both D1-Asp61 and D2-His61 are highly conserved from cyanobacteria to higher plants.

8.4.4. Influences of side-chain and the Mn-cluster on $E_m(P_{D1/D2})$

In PSII, the direct influence of the Mn-cluster on $E_m(P_{D1/D2})$ is an up-shift of ~210-240 mV (Table 8-4-1). This influence is a factor of 2 smaller for the Chl*a* on the D2 side but still significant (~110-150 mV). On the other hand, the net charge of side-chains in PSII down-shifts $E_m(P_{D1})$ by ~120 mV relative to $E_m(P_{D2})$ (Table 8-4-1), giving rise to a partial compensation of the influence from charges of the Mn-cluster. Indeed, in the PSII crystal structure (Loll et al., 2005), the D1 side where the Mn-cluster is located, obviously consists of a smaller (larger) number of basic (acidic) residues than the D2 side; otherwise the Mn-cluster in PSII would have been energetically very unfavorable. Thus, when we compare bRC with PSII, the combined influence of the net charge from Mn-cluster and side-chains results in a much smaller E_m difference of 70-120 mV between $P_{L/M}$ and $P_{D1/D2}$, respectively (Table 8-4-1). Note that the influence on the E_m from the iron-sulfur cluster F_X in PSI or the non-heme Fe-complex in bRC/PSII is very small for these (B)Chl*a* (Ishikita et al., 2005c).

8.4.5. Backbone dipole of His-providing α-helix stabilizes Chla^+ by 130 mV in PSI relative to PSII

The protein backbone induced up-shift of E_m is significantly larger for the Chl*a* in PSII than for the corresponding cofactors in the other two photosynthetic RC (Table 8-4-1). We calculated the direct influence of backbone charges for each secondary structural component in these proteins. Remarkable is the strong influence of the helices D in bRC/PSII. They exhibit considerable backbone up-shifts $E_m(P_{D1/D2})$ by 100 mV and $E_m(P_{L/M})$ by 70-80 mV (Table 8-4-2). Notably, these helices D provide the His-axial ligands to $P_{D1/D2}$ (D1-His198/D2-His197) and $P_{L/M}$ (His-L173/His-M202). On the other hand, the corresponding helices J in PSI (PsaA670-691/ PsaB650-671) yield down-shifts of $E_m(P_{A/B})$ by 28/27 mV, thus giving rise to a difference in E_m(Chl*a*) of ~130 mV between PSI and PSII induced by the protein backbone.

A significant difference of the helices D in PSII from the helices J in PSI are the positions of the His-axial ligands (Figure 8-4-1). In PSII (and also bRC) the His-axial ligands are located at the edge of the helices D, while in PSI they are in the middle of these helices J. Hereby, in PSII only 2 residues (D1-196 and 197/ D2-195 and 196)

precede the His positions (D1-198/D2-197), while in the helices J of PSI ten residues (PsaA670-679/ PsaB650-659) precede the His that are located at PsaA680/ PsaB660.

To investigate the effect of the protein backbone region upstream of the His-ligand position, we removed eight residues in the helices J of PSI (PsaA670-677/ PsaB650-657) that are absent in the corresponding helix regions of PSI and calculate the direct influence of the remaining backbones PsaA678-691/ PsaB658-671 on $E_m(P_{A/B})$. We found that the protein backbone in this region of PSI up-shifts $E_m(P_{A/B})$ by ~100 mV, which is the same value as that calculated for $E_m(P_{D1/D2})$ as a contribution of the backbone of the helices D in PSII (Figure 8-4-1). This, in turn, indicates that the region PsaA670-677/ PsaB650-657 that is absent in PSII down-shifts $E_m(P_{A/B})$ by ~130 mV in PSI (Figure 8-4-1). The down-shift of ~130 mV in $E_m(P_{A/B})$ from the protein backbone region PsaA670-677/ PsaB650-657 originates from the backbone carbonyl group dipoles with carbonyl oxygens oriented toward $P_{A/B}$ (Figure 8-4-1). The influence of backbone amide groups is significantly smaller relative to that of the carbonyl groups. Since these carbonyl group dipoles are absent in PSII (and also in bRC), the $E_m(P_{D1/D2})$ is up-shifted by ~130 mV relative to $E_m(P_{A/B})$. We note that for this part of the helices D there is no significant difference in backbone orientation or disorder between bRC and PSII.

Table 8-4-2. Influence of backbone charges on E_m(Chl*a*) in the D1/D2 core and E_m(BChl*a*) in bRC (PDB: 1AIG) (Stowell et al., 1997) [mV].

	D2		**D1**		**M**		**L**	
	Chl_{D2}	**P_{D2}**	**P_{D1}**	**Chl_{D1}**	**B_M**	**P_M**	**P_L**	**B_L**
helix C	**19**	**23**	**12**	**7**	**–3**	**3**	**0**	**5**
D1 (143-165)/ L (116-138)	3	3	4	2	1	1	–1	3
D2 (147-163)/ M (145-167)	16	20	8	5	–4	2	1	2
lumenal segment CD1	**9**	**–5**	**–2**	**–14**	**–15**	**–14**	**–13**	**–43**
D1 (166-175)/ L (139-151)	0	–2	4	–13	–2	–12	–11	–43
D2 (164-175)/ M (168-178)	9	–3	–6	–1	–13	–2	–2	0
lumenal helix CD	**80**	**38**	**59**	**46**	**10**	**–12**	**–11**	**56**
D1 (176-190)/ L (152-162)	3	21	25	45	–2	9	–9	59
D2 (176-188)/ M (179-192)	77	17	34	1	12	–21	–2	–3
lumenal segment CD2	**1**	**62**	**57**	**–2**	**–11**	**25**	**21**	**–7**
D1 (191-195)/ L (163-170)	–15	12	31	10	–15	10	9	2
D2 (189-194)/ M (193-199)	16	50	26	–12	4	15	12	–9
helix D	**60**	**95**	**95**	**60**	**35**	**84**	**74**	**28**
D1 (196-221)/ L (171-198)	45	21	68	17	24	17	54	8
D2 (195-219)/ M (200-225)	15	74	27	43	11	67	20	20

8.4.6. Protein backbone near lumenal helix up-shifts $E_m(P_{D1/D2})$ by 90-110 mV in PSII relative to $E_m(P_{L/M})$ in bRC

For PSII and bRC the backbone of the two helices D providing the His-ligands of $P_{D1/D2}$ and $P_{L/M}$ have essentially the same impact on $E_m(P_{D1/D2})$ and $E_m(P_{L/M})$ (difference of only 10-20 mV) (Table 8-4-2), while the total backbone influence on $E_m(P_{D1/D2})$ and $E_m(P_{L/M})$ yields a difference of 100-160 mV (Table 8-4-1). We found that 90-110 mV of this 100-160 mV E_m difference originates from the backbone of the helix segments D1-176-195/D2-176-194 in PSII and L152-170/M179-199 in bRC, i.e. the lumenal

helices CD and the adjacent linker segments to the helices D (Table 8-4-2). Indeed, this region of PSII has been proposed to play an important role in the energetics of $P680^+$ (Manna et al., 1998; Mulkidjanian, 1999; Keilty et al., 2001).

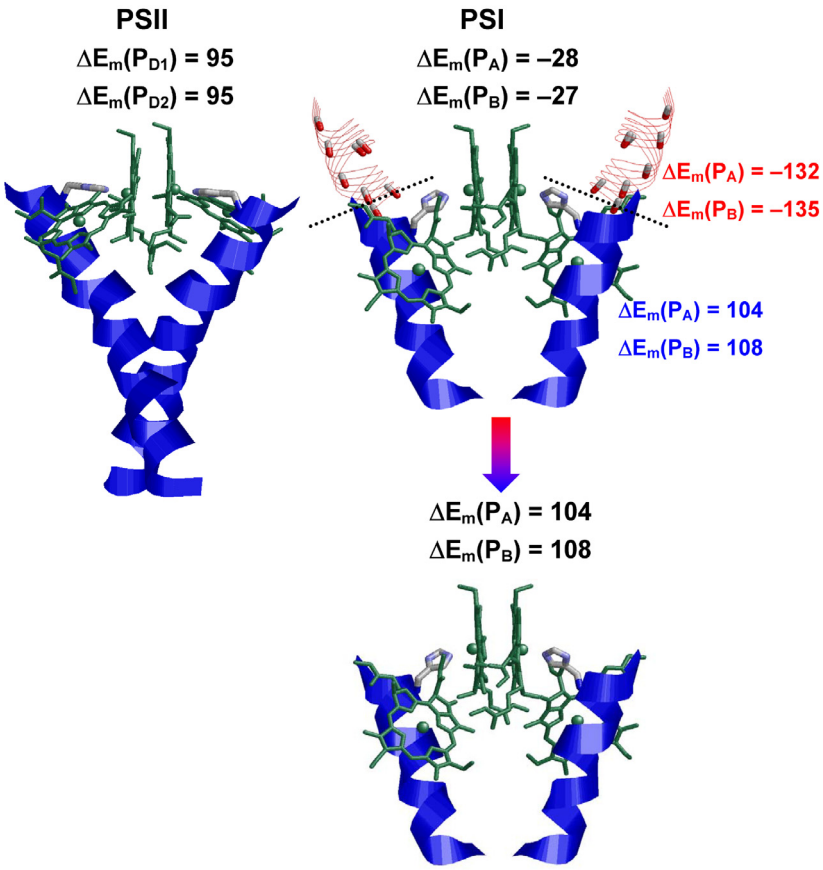

Figure 8-4-1. Different geometries of the helices that provide the His axial ligands to $P_{A/B}$ in PSI (right part) or to $P_{D1/D2}$ in PSII (left part). ΔE_m indicates the direct influence of backbone charges on either $E_m(P_{A/B})$ or $E_m(P_{D1/D2})$. The carbonyl groups of the eight residues in the corresponding helix J of PSI (PsaA670-677/ PsaB650-657) are shown explicitly (red for oxygen, white for carbon). The lower right part depicts the situation in PSI where the helices were shortened by these eight residues to model the arrangement in PSII. Values of the direct influence of backbone charges on the removed and remaining parts of the helices are colored in red and blue, respectively.

Helix CD_{D1} of PSII (D1-176-190) is four residues longer (D1-187-190) than helix CD_L of bRC (L152-162), while helix CD_{D2} (D2-176-188) and helix CD_M (179-192) possess essentially the same length (Figure 8-4-2, left). This structural difference in the length of helix CD_{D1} is probably related to the presence of the Mn-cluster on the D1 side, to which D1-Glu189 at the C-terminal edge of the CD_{D1} helix ligates (Figure 8-4-2, left). We calculated the direct influence of the backbone for these four extra residues D1-187-190, and found up-shifts of $E_m(P_{D1/D2})$ by 48/22 mV.

In addition, there are other significant differences in this region between bRC and PSII: (i) in PSII D1-His190/D2-His189 (at/near the C-terminal edge of the helices $CD_{D1/D2}$) are H-bond partners for the redox-active tyrosine $Y_{Z/D}$ (D1-Tyr161/D2-Tyr160) from the same helices (Figure 8-4-2, left) (ii) in bRC His-L153/M182 near the N-terminal edge of helices $CD_{L/M}$ are axial ligands for $B_{L/M}$, while in PSII the corresponding $Chl_{D1/D2}$ possess no axial ligands (Figure 8-4-2, right). All these significant structural features in this region are likely responsible for the different backbone coordination between bRC and PSII, resulting in a net E_m difference

of 90-110 mV between $P_{D1/D2}$ and $P_{L/M}$.

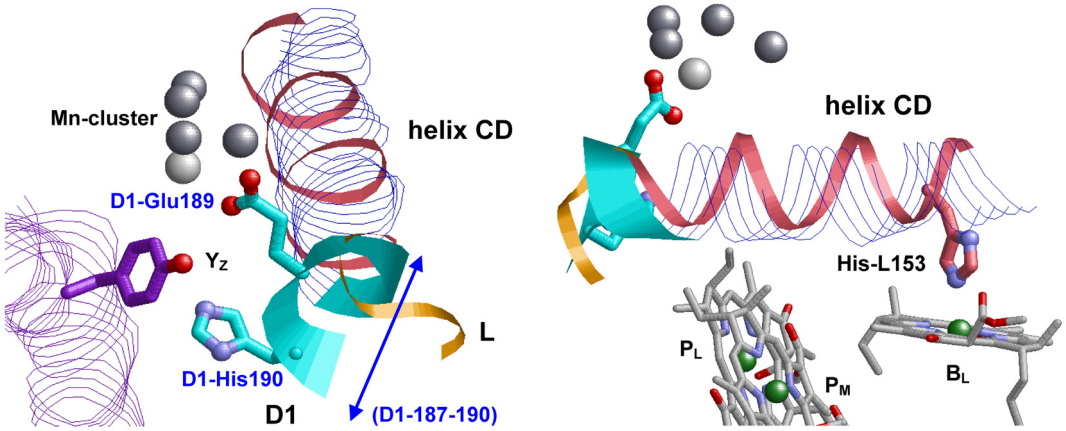

Figure 8-4-2. Lumenal/periplasmic helix CD in bRC and PSII. The helices are depicted with ribbon/strand model for bRC/PSII. Region D1-187-190 in PSII is depicted as wide ribbon model. a) Extension of the helix CD on the D1 side of PSII (D1-187-190) with respect to bRC. b) Ligation of His-L153 from the CD helix to B_L in bRC. The corresponding His residue is absent in the helix CD of PSII.

Conclusion I: E_m difference of 600 mV between $P_{D1/D2}$ and $P_{A/B}$

The calculated $E_m(P_{D1/D2})$ for the complete PSII complex are 1200-1220 mV. These values decrease by 110-130 mV in the D1/D2/CP43/CP47 core. Upon deletion of CP43/CP47 (i.e. forming the D1/D2 core), the $E_m(P_{D1/D2})$ decreases furthermore by another 60-70 mV yielding +1020-1030 mV, which is still considerably high. Hence, the protein subunits peripheral to D1/D2 up-shift $E_m(P_{D1/D2})$ by 170-200 mV**.** This contrasts with PSI where the calculated $E_m(P_{A/B})$ in both the complete PSI complex and the PsaA/PsaB core are +590-600 mV.

Elimination of the atomic charges in the D1/D2 core (PSII) yields $E_m(P_{D1/D2})$ = +710-720 mV. Elimination of the atomic charges in the PsaA/PsaB core (PSI) yields essentially the same $E_m(P_{A/B})$ of +710-720 mV, indicating that **the protein dielectric volumes of the D1/D2 and PsaA/PsaB cores do not result in different E_m(Chl*a*).**

The atomic charges in the D1/D2 core up-shift $E_m(P_{D1/D2})$ by 300-330 mV, while those in the PsaA/PsaB core, in turn, down-shift $E_m(P_{A/B})$ by 100-130 mV. As a consequence, the **atomic charges differentiate between $E_m(P_{A/B})$ and $E_m(P_{D1/D2})$ by 400-450 mV.** Especially, the **charges of the Mn-cluster up-shift $E_m(P_{D1/D2})$ by 210/100 mV.**

Relative to $E_m(P_{A/B})$ the protein backbone charges up-shift $E_m(P_{D1/D2})$ by 150-180 mV. Most remarkable are the different geometries of the α-helices that provide the His-ligands for $P_{D1/D2}$ or $P_{A/B}$. **The dipoles of the backbone carbonyl groups at the eight residues (PsaA670-677 / PsaB650-657) in the α-helices J of PSI** (that are absent in the α-helices D of PSII) **stabilize Chla^+ in PSI dramatically, giving rise to 130-140 mV down-shift in $E_m(P_{A/B})$ relative to $E_m(P_{D1/D2})$.** In this regard, in bRC the corresponding α-helices have the same influence on $E_m(P_{L/M})$ as have the helices D in PSII on $E_m(P_{D1/D2})$.

Conclusion II: E_m difference of 600 mV between $P_{L/M}$ and $P_{D1/D2}$

The calculated $E_m(P_{L/M})$ is +640-660 mV. This is consistent with the experimental value of +640 mV for the heterodimer bRC, which is generally assumed to yield the E_m for the uncoupled monomeric BChl*a* at this site. However, the E_m(P870) is lower by 140-160 mV presumably due to electronic coupling between P_L and P_M.

The peripheral subunits of the D1/D2 core (PSII) up-shift $E_m(P_{D1/D2})$ by 170-200 mV, while no corresponding shift is found for bRC that does not possess those subunits.

The remaining 160 mV of the 600 mV difference are due to different reference-solvent E_m values between Chl*a* and BChl*a* (with CH_2Cl_2 as solvent in the present study).

Relative to $E_m(P_{L/M})$, the backbone charges up-shift $E_m(P_{D1/D2})$ by 100-160 mV. The major part of this difference **(90-110 mV) originates from the lumenal/periplasmic segments D1-176-195/ D2-176-194 in PSII and L152-170/ M179-199 in bRC.** These parts involve significant structural differences between bRC and PSII: (i) the presence of D1-Glu189 as ligand for the Mn-cluster in PSII, (ii) His-L153/M182 as axial ligands for $B_{L/M}$, which are lacking for $Chl_{D1/D2}$ in PSII, and (iii) D1-His190/D2-His189 as H-bond partners for $Y_{Z/D}$ (D1-Tyr161/D2-Tyr160), which are lacking in bRC.